OTX2 Transcription Factor Controls Regional Patterning Within The Medial Ganglionic Eminence (MGE) And Regional Identity Of The Septum

Renée V. Hoch[1], **Susan Lindtner**, **James D. Price**, and **John L.R. Rubenstein**[*]

Department of Psychiatry, University of California, San Francisco, CA, 94143, USA

Summary

The *Otx2* homeodomain transcription factor is essential for gastrulation and early neural development. We generated *Otx2* conditional knockout (cKO) mice to investigate its roles in telencephalon development after neurulation (~E9.0). We conducted transcriptional profiling and in situ hybridization to identify genes de-regulated in *Otx2* cKO ventral forebrain. In parallel, we used ChIP-seq to identify enhancer elements, the OTX2 binding motif, and de-regulated genes that are likely direct targets of OTX2 transcriptional regulation. We found that *Otx2* was essential in: septum specification, regulation of Fgf signaling in the rostral telencephalon, and medial ganglionic eminence (MGE) patterning, neurogenesis, and oligodendrogenesis. Within the MGE, *Otx2* was required for ventral but not dorsal identity, thus controlling the production of specific MGE derivatives.

Graphical abstract

[*]Corresponding author john.rubenstein@ucsf.edu Ph: 415-476-7862 FAX: 415-476-7884.
[1]Current address: PLOS, 1160 Battery Street, San Francisco, CA, 94111, USA
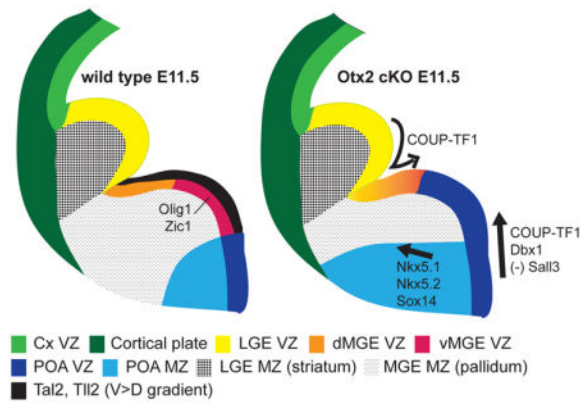
wild type E11.5 / Otx2 cKO E11.5

COUP-TF1

Olig1/ Zic1

COUP-TF1
Dbx1
(-) Sall3

Nkx5.1
Nkx5.2
Sox14

■ Cx VZ ■ Cortical plate ■ LGE VZ ■ dMGE VZ ■ vMGE VZ
■ POA VZ ■ POA MZ ▦ LGE MZ (striatum) ░ MGE MZ (pallidum)
■ Tal2, Tll2 (V>D gradient)

INTRODUCTION

Otx2 is one of two mammalian orthologs of the Drosophila homeodomain transcription factor (TF), Orthodenticle. *Otx2* is essential in the visceral endoderm during gastrulation for specification of anterior neuroectoderm, where it induces early forebrain-specific genes (Acampora et al., 1995; Rhinn et al., 1998; Tian et al., 2002). Telencephalic expression of *Otx2* continues in the rostral patterning center (RPC; septal anlage), ventral telencephalon (subpallium; ganglionic eminences), and caudodorsal telencephalon (including choroid plexus; Figure 1; (Simeone et al., 1992)). Abrogation of *Otx2* function after early neurulation through enhancer deletion showed that *Otx2* maintains forebrain identity after its specification, and is required later in the caudodorsal telencephalon for medial pallial morphogenesis (Kurokawa et al., 2004a; Kurokawa et al., 2004b; Sakurai et al., 2010).

Otx2 roles in the RPC and ventral telencephalon have not been reported. The RPC is a source of Fgfs (Fgf8, 17, 18) with essential roles in forebrain growth and patterning (Martinez et al., 1999; Crossley et al., 2001; Fukuchi-Shimogori and Grove, 2001; Chi et al., 2003; Storm et al., 2006; Cholfin and Rubenstein, 2007; Grove and Monucki, 2013). Notably, *Otx2* expression also abuts the midbrain/hindbrain boundary (MHB) patterning center, which secretes the same array of Fgfs to help instruct development of midbrain/ hindbrain structures (Simeone et al., 1992; Martinez et al., 1999; Chi et al., 2003).

Otx2 may be involved in regulating and responding to FGFs from the RPC and MHB. FGF8 bead implantation in prosencephalon, mesencephalon, and optic vesicle tissue indicated that FGF8 represses *Otx2* expression (Martinez et al., 1999; Crossley et al., 2001). Conversely, there is evidence for *Otx2* regulation of *Fgf8* expression: reduced *Otx2* expression results in anterior expansion of *Fgf8* expression in the MHB (Acampora et al., 1997; Puelles et al., 2003).

Otx2 is expressed in the septal primordium (Se), the ganglionic eminences (GEs: MGE, LGE, CGE), and the preoptic area (POA; Figure 1). The MGE gives rise to the globus pallidus (GP) and to striatal and cortical interneurons (Flandin et al., 2010; Rubenstein and Campbell, 2013). The LGE gives rise to striatal neurons and olfactory bulb interneurons (Rubenstein and Campbell, 2013). The CGE gives rise to cortical interneurons (Batista-Britto and Fishell, 2013). The POA gives rise to preoptic nuclei and some of the amygdala and cortical interneurons (Hirata et al., 2009; Gelman et al., 2011). Fate mapping demonstrated that *Fgf8*^{+} ventral MGE and ventral Se progenitors generate cholinergic neurons of the basal ganglia (Hoch et al., 2015,). In addition to their neuronal derivatives, the embryonic MGE, LGE, and POA also generate oligodendrocytes that populate the basal ganglia and cortex (Kessaris et al., 2006).

The GEs are subdivided into molecularly and functionally distinct progenitor subdomains along the dorsoventral (D-V) axis that give rise to different subclasses of neurons (Flames et al., 2007; Flandin et al., 2010; Waclaw et al., 2010). Factors that establish these progenitor subdomains are unknown.

We used conditional mutagenesis to elucidate roles of *Otx2* in the ventral forebrain and septum. These analyses revealed novel telencephalic roles of *Otx2*. In the RPC, *Otx2* restricted *Fgf8* and *17* expression along the rostral-caudal and D-V axes, and controlled Fgf-signaling through feedback regulation of *Sprouty* expression in the RPC, MGE and POA. In the GEs, *Otx2* promoted MGE neurogenesis and oligodendrogenesis, and controlled MGE sub-regional identity. Based on mRNA expression changes and OTX2 ChIP-seq data, we propose molecular mechanisms how *Otx2* patterns MGE regional subdivisions.

RESULTS

Conditional mutagenesis of *Otx2* in the telencephalon

In the E11.5 telencephalon, *Otx2* is expressed in the ventricular zone (VZ) of the Se, GEs, POA, choroid plexus, and hippocampal anlage (Figure 1A–A"). To investigate Otx2 functions in the telencephalon, we conducted conditional mutagenesis experiments using *Otx2*[f] mice (Tian et al., 2002). We used two Cre deleter alleles to abrogate Otx2 expression after gastrulation: *RxCre*, in which Cre is expressed in the telencephalic neural plate anlage (~E8.5; (Swindell et al., 2006)), and *Nkx2.1Cre*, in which Cre is expressed in the MGE, POA, and ventral Se (vSe) beginning around E9.5 (Xu et al., 2008).

We used immunohistochemistry (IHC) and in situ hybridization (ISH) to evaluate levels of protein and mRNA in *Otx2* cKOs. Anti-OTX2 IHC showed that OTX2 protein expression was lost throughout the telencephalon in *RxCre* cKOs by E11.5, except in caudal dorsomedial structures (Figure 1C–F; arrows in C'-C" and D'-D" indicate maintained protein expression). Anti-OTX2 IHC confirmed that *Nkx2.1Cre* cKOs lacked OTX2 expression in the E11.5 MGE (Figure 1G–H).

ISH using a full-length *Otx2* probe detected increased levels of the mutant transcript in *RxCre* cKOs, suggesting that conditional deletion of *Otx2* leads to increased state-steady levels of *Otx2* transcripts (Figure 1A–A", B–B"), particularly in the MGE VZ and in the

caudal MGE subventricular zone (SVZ; arrowheads, Figure A', B', and arrows, Figure 1A", B").

We performed OTX2 ChIP-seq three times from E12.5 wild type subpallium (described below in more detail). A ChIP-seq peak is presumptive evidence for OTX2 *in vivo* binding and possible function at this locus. We observed multiple ChIP-seq peaks near the *Otx2* locus (Figure 2K). These data suggest that Otx2 negatively autoregulates its expression.

Otx1 is also expressed in the developing forebrain (Simeone et al., 1992). *Otx1* and *Otx2* had complementary expression patterns in the E11.5 telencephalon: *Otx2* is expressed strongly in the subpallial VZ, whereas *Otx1* is expressed predominantly in the pallial VZ and dorsal LGE, but is expressed at lower levels in the GEs (Figures 1A–A" and Figure S1A–C). Notably, *Otx1* and *Otx2* are expressed in the SE, LGE, caudal MGE, and dorsomedial cortical structures (Figures 1A–A", asterisks in Figure S1A–C). *Otx1* mRNA expression was not demonstrably altered in $Otx2^{f/-}$; *RxCre* embryos at E11.5, (Figure S1B).

RxCre E11.5 cKOs had hypoplastic MGEs, with reductions in the SVZ and marginal zone (MZ; asterisks, Figure 1A', B'). We conducted an RNA expression microarray experiment using RNA from control and *RxCre* cKO Se, MGE, and LGE (GEO accession number: GSE69727). This analysis identified 139 significantly deregulated genes (including those discussed in the results: Table S1). In parallel, we used microdissected subpallium (septum, MGE, and LGE) from wild type E12.5 embryos in three independent anti-OTX2 ChIP-seq experiments (Figure 2, data not shown)(GEO accession number: GSE69727). By comparing microarray and ChIP-seq datasets, we developed hypotheses as to which genes are direct targets of OTX2 that mediate its functions in the RPC and GEs.

Otx2 impacts Fgf signaling in the RPC and is required for septum specification

RxCre cKO telencephalons also are hypoplastic along the rostrocaudal axis at E11.5: the rostral pole>caudal septum distance was 528 +/− 32 μm in $Otx2^{f/+}$ embryos (n=4) and 294 +/− 97 μm in $Otx2^{f/-}$; *RxCre* embryos (n=5). *Fgf8* and *Fgf17* mRNA expression domains expanded rostrally and ventrolaterally into the MGE at E11.5 (arrowheads Figure 3A–E). Thus, *Otx2* restricts RPC Fgf signaling. *Fgf8* hypomorphs had reduced *Otx2* expression in the rostral telencephalon (Figure S2A–B, (Storm et al., 2006)). Thus, *Otx2* and *Fgf8* function and expression are tightly coordinated.

FGF signaling induces the expression of negative feedback inhibitors, including *Sprouty1, Sprouty2,* and *MAP Kinase Phosphatase 3 (Mkp3*, also called *Dusp6*; (Minowada et al., 1999; Eswarakumar et al., 2005; Thisse and Thisse, 2005; Faedo et al., 2010). These genes were deregulated in *RxCre* cKOs. *Sprouty1* expression was diminished in the POA (Figure 3F–G'). *Sprouty2* was upregulated in the RPC, MGE, and LGE (Figure 3H–I'), and *Mkp3* was upregulated in the MGE (Figure 3J–J', N-N'). Anti-OTX2 ChIP-seq data provided evidence that *Fgf8*, *Sprouty1*, *Sprouty2*, and *Mkp3* were direct targets of OTX2 (Figure 2E, P, Q). We did not observe reproducible ChIP-seq peaks for *Fgf17*. Thus, Otx2 regulates FGF signaling in the Se and GEs in several ways.

Fgf8 and *Fgf17* establish gradients of gene expression that pattern the cortical primordium (Fukuchi-Shimogori and Grove, 2001; Garel et al., 2003; Cholfin and Rubenstein, 2007). *RxCre* cKOs at E13.5 had altered dorsoventral gradients of *COUP-TF1* and *Sp8*. *COUP-TF1* expression was downregulated in the dorsal cortex (Figure S2C–D). Conversely, *SP8* was upregulated in the dorsal and medial cortex and its graded expression extended further ventrally (Figure S2E–F). These changes are predictable consequences of increased Fgf8 signaling (Garel et al., 2003; Storm et al., 2006).

The RNA expression microarray identified two midbrain/hindbrain genes, *En2* and *Pax3*, which were upregulated in *RxCre* cKO telencephalons (Figure 3K–M', O-Q'; see also Allen Brain Atlas). Normally, *En2* is highly expressed around the MHB (Liu and Joyner, 2001). *Pax3* is expressed in the midbrain and hindbrain at E11.5 ((Goulding et al., 1991); Allen Brain Atlas). Both *En2* and *Pax3* were ectopically expressed in the RPC/Se and medial PFC (Figure 3K–M', O–Q'). Notably, we detected low levels of *Pax3* in a small subdomain of the caudal RPC in control forebrains (Figure 3Q). We did not detect ChIP-seq peaks near the *En2* locus, but *Pax3* had two strong intragenic peaks (Figure 2L), suggesting that this is a direct OTX2 target. Ectopic/elevated expression of *En2* and *Pax3* suggests that Se progenitors are mis-specified.

Otx2 is required for early oligodendrogenesis in the basal ganglia

The bHLH TFs *Olig1* and *Olig2* were downregulated in the E12.5 RNA microarray experiment (Table S1). ISH at E11.5 confirmed that *Olig1* was reduced throughout the caudal MGE and POA VZ, and *Olig2* was selectively downregulated in the ventral subdomains of these structures (Figure 4B–C', E–F'). At E13.5, *RxCre* cKOs had reduced *Olig1* expression in the Se and MGE VZ, and fewer scattered *Olig1+* immature oligodendrocytes in the MZ (Figure 4G–I'). E12.5 ChIP-seq data revealed numerous OTX2 binding sites in the vicinity of the *Olig1/Olig2* locus (Figure 2N), suggesting these two genes are direct targets of OTX2 regulation.

Olig1 expression in *Nkx2.1Cre* cKOs was slightly reduced in the vMGE and POA at E11.5 (not shown). At E13.5, *Olig1* expression in the Se VZ appeared normal, but was strongly reduced in the caudal MGE VZ, and there were fewer scattered *Olig1+* cells in the MZ (not shown). Thus, *Otx2* is required in the early MGE VZ for oligodendrogenesis.

Otx2 is required in the MGE for progenitor specification and neurogenesis

The GEs of *RxCre* cKOs were hypoplastic at E11.5 (Figure 4B–B', Figure 5). We examined E11.5 expression of *Dlx1*, a homeobox gene expressed mosaically in the MGE and LGE VZ, homogeneously in their SVZs, and in differentiating neurons.. *Dlx1* expression was reduced in the VZ, SVZ and MZ (Figure 5A', B'). OTX2 binds to two enhancers in the *Dlx1/2* locus (I12b and URE2) that are active in the embryonic subpallium (Figure 2D; S5G–J)(Ghanem et al., 2007). This phenotype was also observed in *Nkx2.1Cre* cKOs (Figure 5B, B'), suggesting that Otx2 participates in MGE neurogenesis.

In support of this model, several markers of differentiating MGE neurons were downregulated (Table S1). For example *Arx* RNA was reduced ~1.7-fold in the microarray.

OTX2 ChIP-seq peaks were identified near *Arx* (Figure 2A), including at two enhancers with subpallial activity (Figure S5A–D)(Ahituv et al., 2007; Colasante et al., 2008; Visel et al., 2013). At E11.5, *Arx* was expressed in MGE VZ, SVZ and MZ (Figure 5C), but was reduced in the *RxCre* cKOs (Figure 5C'). Similarly, *Shh* (MGE MZ), *PlxnA4* (MGE and LGE SVZ/MZ) and *Gbx2* (MGE MZ) expression was reduced (Figure 5M–N', and data not shown). All three OTX2 ChIP-seq experiments detected OTX2 peaks on a *Shh* enhancer that promotes MGE expression (SBE4) (Jeong et al., 2006).

Markers of immature MGE-derived interneurons, including *Lhx6*, *c-maf*, *Somatostatin*, *NPY*, and *Gad1*, were also downregulated (Table S1). Furthermore, neurogenesis in the E11.5 MGE was reduced, as indicated by IHC to the pan-neuronal marker, β-III-tubulin (Tuj1 antibody)(Figure 5D–D').

Unlike *Arx*, β-III-tubulin and *Dlx1*, which were moderately reduced in the cKOs, expression of *Robo2* was barely detectable (Figure 5E–F'). *Nkx2.1Cre* cKOs exhibited a similar phenotype (Figure 5G–H'). Several ChIP-seq peaks were identified ~1MB from the *Robo2* locus, within the *Robo1* locus (Figure 2M).

We next examined proliferation in the E11.5 MGE of the *RxCre* cKO using IHC to phosphohistone H3 (pH3). pH3$^+$ cells were strongly reduced in the SVZ (Figure 5I–J arrowheads), while the VZ did not show a clear phenotype. In considering the mutant's neurogenesis deficit, and the reduction of mitotic SVZ (pH3$^+$) cells, we were intrigued that anti-neurogenic factors *Hes1* and *Id4* were both upregulated in the E12.5 *RxCre* microarray (Table S1). *Hes1* and *Id4* are expressed in dorsal>ventral gradients in the MGE VZ at E11.5; these gradients were lost, as these genes were upregulated throughout the MGE (Figure 5K–L'). ChIP-seq data indicated that *Otx2* binds genomic DNA near the *Hes1* locus and may also bind near the *Id4* locus (Figure 2F, H).

Together, these data support a model in which *Otx2* directly regulates genes that control the generation and differentiation of MGE-derived neurons. *Otx2* represses inhibitors of MGE differentiation (*Hes1* and *Id4*), and thus, loss of *Otx2* function results in reduced production of SVZ progenitors and neurons. Furthermore, *Otx2* promotes neuronal maturation by positively regulating *Arx* and *Dlx1* expression, genes that support the differentiation of MGE-derived neurons.

Otx2 specifies vMGE fate and repress POA fate

Olig2, *Fgf*, and *Sprouty1* expression changes in *RxCre* cKOs indicated that the vMGE and POA were particularly affected by the loss of *Otx2*. Thus, we hypothesized that *Otx2* may play a role in regional specification of the basal ganglia. To investigate this, we examined microarray data (Table S1) for expression changes relevant to MGE and POA patterning, and performed ISHs at E11.5. Multiple genes that had restricted expression in the POA (progenitors and/or neurons) were upregulated (Table S1); ISH revealed that their expression expanded rostrally and/or dorsally into the ventral MGE (vMGE). These "POA genes" included *Nkx5.2*, *Dbx1*, *Slit2*, *Arhgap22*, *Sox3*, *Sox14*, and *mShisa* (Figure 6A–C, D–F, H–M, and data not shown). Conversely, several MGE markers were identified as downregulated on the microarray (Table S1). ISHs validated these results and demonstrated

that the *RxCre* cKO MGE VZ failed to express *Tal2* and *Tll2*, which are novel markers of the vMGE (Figure 6N–Q). Furthermore, *Sall3* was downregulated within the vMGE VZ (Figure 6R–S), and *Tgfb3* was downregulated in the vMGE SVZ (Figure 6G). *COUP-TF2*, which is strongly expressed in the CGE and dMGE of wild type E11.5 embryos, was overexpressed in the vMGE VZ and SVZ of *Otx2* cKOs (data not shown); this could reflect a rostral and/or ventral shift in this gene's expression domain. Together, these findings (summarized in Figure S7) provide evidence that *Otx2* patterns MGE regional identity by specifying vMGE properties and by repressing POA identity.

Importantly, ChIP-seq data revealed OTX2 binding peaks in or near several downregulated MGE genes (Tal2, Tll2, Sall3)(Figures 2O,R,S; S5K,L). In contrast, most upregulated POA genes, including *Nkx5.2*, *Slit2*, *Arhgap22*, and *Sox3*, did not have nearby OTX2 binding peaks (Figure 2 and data not shown). One notable exception was *Dbx1*, a POA marker that had OTX2 ChIP-seq peaks (Figure 2C). Furthermore, OTX2 occupied enhancer elements, with subpallial activity at E11.5, near genes with reduced expression in the *Otx2 RxCre* cKOs (*Arx, Dlx1&2* and *Sall3*; Figure S5). These data support a model in which Otx2 patterns the basal ganglia by direct, positive transcriptional regulation of MGE genes, and by repressive effects on POA gene expression that are predominantly indirect (Figure S7).

At E13.5, *RxCre* cKOs phenotypes continue to demonstrate expansion of POA identity into the MGE. *Nkx5.1* expression, which is normally restricted to a POA SVZ subdomain and a subset of POA MZ cells, expanded dorsally and rostrally (Figure 7A–C and data not shown). *COUP-TF1* is normally expressed in the LGE VZ, the POA VZ and MZ, and in a dorsal>ventral gradient in the caudal MGE VZ (Figure 7D,E). In cKOs *COUP-TF1* had increased expression MGE MZ and was ectopically expressed in the caudal MGE MZ (Figure 7D', E'). ChIP-seq data suggest that *COUP-TF1* may be directly regulated by OTX2 (Figure 2). *Zic1* is a marker of the vMGE VZ, the GP, and a subset of other MGE MZ cells at E13.5 (Figure 7G–I). In cKOs *Zic1* was not detectable in the vMGE VZ or GP, and labeled fewer MGE MZ cells (Figure 7G'–I'). ChIP-seq data revealed multiple peaks near the *Zic1* locus (data not shown) suggesting direct regulation by OTX2. GP hypoplasia in *RxCre* cKOs was confirmed by *Nkx2.1* and *ER81* ISH at E13.5, and with *ER81* and *NPAS1* ISH at P0 (Figure 7F, K, data not shown). *Nkx2.1Cre* cKOs at E13.5 exhibited similar, though less severe POA and MGE phenotypes (Figure S3).

While the ventral MGE had the clearest patterning defects in *RxCre* cKOs, we also observed subtle deficits in the dorsal MGE. At E13.5, transcriptional co-activator *Sizn1* (MGI nomenclature: *Zcchc12*) is expressed in the VZ of the ventral LGE (Figure 7N, O). In cKOs, *Sizn1* expression extended ventrally into dMGE (Figure 7N', O'); we did not observe OTX2 ChIP-seq peaks near *Sizn1*, suggesting this was an indirect effect of Otx2 functions.

Although *Otx2* is expressed in the VZ of the LGE and MGE, the LGE had only a mild phenotype in *RxCre* cKOs at E11.5, E13.5 and P0. For example, *Ikaros*, which labels neurons in the MZ of the LGE (striatum), was expressed in the normal domain, albeit at lower levels, at E15.5 (Figure 7M).

Otx2 regulates development of interneurons and cholinergic neurons derived from the MGE and POA

The MGE and POA give rise to cortical and striatal interneurons and basal ganglia cholinergic neurons, as such *RxCre* cKOs affected these neurons. *Lhx6* and *Lhx8* expression were reduced in these regions (Figure S4A'–C'). *Lhx8*+ striatal interneurons were reduced (Figure S4D–F'). *Lhx6* and *c-maf* ISHs suggested that *RxCre* cKOs may have reduced numbers of cortical interneurons at P0 (Figure 8A–C', data not shown). However, at P13-15 we did not observe significant changes in somatostatin and parvalbumin IHC-positive cortical interneuron numbers (data not shown).

~80% of cholinergic neurons in the basal ganglia originate in the vMGE and septum from RPC-derived progenitors (Hoch et al., 2015). As this domain was severely affected in *RxCre* cKOs, we examined cholinergic neurons numbers. *Gbx1* and *TrkA* are expressed in basal ganglia cholinergic neurons at P0 (Asbreuk et al., 2002; Sanchez-Ortiz et al., 2012); both markers were reduced in the mutants (Figure S4G–I'), as were ChAT+ neurons at P13–P15 (Figure S4J–L'). *Nkx2.1Cre* cKOs exhibited a milder reduction of ChAT+ neurons (Figure S3J–L').

Bioinformatics identifies OTX-binding motifs

OTX2 ChIP-seq was performed three times from E12.5 subpallium. Replica #1 had 995 peaks, replica #2 had 1416 peaks and replica #3 had 19881 peaks (Figure S5M). We focused on ChIP-seq peaks present in all three replicas, yielding 590 regions (Figure S5M), which were analyzed Regulatory Sequence Analysis Tools (RSAT) (Thomas-Chollier, et al., 2011). Four variations of a frequently detected motif were assigned to CRX [GGATTA (TAATCC)] by the JASPAR database. CRX and OTX2 both have bicoid homeodomains that bind to the same motif (Zhang et al., 2002). 269/590 of the OTX2 ChIP-seq peaks (45.6%) had the core binding sequence GGATTA. These regulatory domains also had motifs for other homeodomain proteins [HOXA5/PDX1 (36%) or NOBOX (12.5%)], and for HMG box proteins, (e.g. SOX2 motifs; 32%) (Figure S6A). 53% of OTX2 motif-containing enhancers had either the other homeodomain or HMG box motifs; 61% of OTX2 motif-negative enhancers did not have either of these motifs.

Several of the dysregulated genes in the *Otx2* mutants had OTX2 ChIP-seq peaks (Figure 2); those with OTX2 motifs have yellow stars in Figure 2. In some cases, broad domains of OTX2 binding lacked the OTX2 motif (e.g. in the *Dlx1/2, Dbx1, Mpk3* loci), suggesting that OTX2 binding in these cases may be through protein-protein interactions.

Gene ontologies (GO) were computed using the GREAT tool (McLean et al., 2010)(Figure S6B). The most frequent GO molecular function terms showed that OTX2 target genes were highly enriched for transcription regulators. The most frequent GO biological function terms showed OTX2 target genes were highly enriched for regulators of neural development. Thus, ChIP-seq analysis on E12.5 ganglionic eminences provided strong support for OTX2 binding *in vivo* to regulatory elements containing the OTX consensus sequence near genes that regulate transcription.

DISCUSSION

Using transcriptional profiling and conditional mutagenesis with two Cre alleles, we demonstrated that *Otx2* regulates: 1) RPC identity and signaling, 2) specification of the vMGE, and 3) promotes MGE neurogenesis and oligodendrogenesis. OTX2 ChIP-seq provided evidence that a subset of genes deregulated in cKOs were direct transcriptional targets of OTX2. To our knowledge, this is the first report of a genome-wide TF ChIP-seq analysis from embryonic basal ganglia. It enabled us to deduce the *in vivo* binding site motifs for OTX2 (Figure S6), to provide evidence for the other TFs that bind in adjacent regions (Figure S6), and to make predictions about which domains have OTX2 binding that do not depend on its association with the OTX2 core motif.

Otx2 specifies rostral patterning center (RPC) identity

Otx2 plays pivotal roles in the early specification of the forebrain and midbrain (Ang et al., 1996; Suda et al., 1996; Acampora and Simeone, 1999), and, at later stages, in midbrain/hindbrain patterning and differentiation (Joyner et al., 2000; Simeone, 2000; Puelles et al., 2003; Vernay et al., 2005; Sakurai et al., 2010). Here we show using *RxCre* that *Otx2* expression after E8.5 is required for specifying RPC function and identity based on: 1) *Fgf* expression domains were expanded, and 2) genes expressed in the MHB patterning center (*Pax3*, *En2*) were ectopically expressed in the RPC (Figure 3). In the developing midbrain, ectopic *Pax3* can induce transcription of *Fgf8*, *En2*, and *Pax3* (Matsunaga et al., 2001). OTX2 ChIP-seq identified two *Pax3* intragenic peaks (Figure 2L); no peaks were found near *En2*. These data suggest that direct repression of *Pax3* by OTX2 is required to inhibit *En2* expression and restrict *Fgf8* and *Pax3* expression in the RPC. This may be a crucial step in defining the identity of the Se, and/or in distinguishing forebrain and midbrain/hindbrain fates. Misspecification of the Se likely contributes to Se hypoplasia (Figure S4J') and reduction in Se cholinergic neurons (Figure S4G–L').

FGF8-bead experiments demonstrated that FGF8 represses *Otx2* expression (Martinez et al., 1999; Crossley et al., 2001). Furthermore, Fgf8 gain of function studies show that increased Fgf8 represses growth (Crossley et al., 2001; Assimacopoulos et al., 2012) that is consistent with the hypoplastic rostral telencephalon (Figure 3A–E). Furthermore, *Otx2* cKO and *Fgf8* hypomorph analyses revealed that *Otx2* spatially restricts *Fgf8* to the RPC (Figure 3A–D), whereas *Fgf8* positively regulates Otx2 in the early rostral telencephalon (Figure S2 A, B; Storm et al., 2006). These data support a model in which *Fgf8* and *Otx2* regulation are interdependent. Indeed*, Otx2* controls feedback regulators of Fgf signaling (*Spry1*, *Spry2*, *Mkp3*) (Figure 3F–J). ChIP-seq data suggest that *Fgf8*, *Spry1*, *Spry2*, and *Mkp3* are direct OTX2 targets (Figure 2). Deregulated Fgf signaling in *Otx2* mutants likely contributes to deficits in cell populations that arise from, or adjacent to, the RPC.

Otx2 promotes neurogenesis and oligodendrogenesis in the MGE

Otx2 expression in the E9.5–E12.5 subpallium is restricted to the VZ and SVZ (Figure 1A–A"), where in the MGE it is required to generate normal numbers of SVZ progenitors and MZ neurons (Figure 5). *Otx2* cKOs overexpress anti-neurogenic TFs (*Hes1*, *Id4*; Table S1; Figure 5) that inhibit neurogenic TFs such as *Ascl1* (*Mash1*) (Casarosa et al., 1999; Yun et

al., 2002). Furthermore, *Otx2* promotes oligodendrogenesis through positive regulation of *Olig1* and *Olig2* (Figure 4)(Petryniak et al., 2007; Silbereis et al., 2014). These mechanisms for neurogenesis and oligodendrogenesis appear to be mediated by direct binding of OTX2 at genomic loci of key regulatory TFs (Figure 2). Later, compensatory mechanisms may rescue these phenotypes as neurogenesis has improved by E13.5–E15.5 (Figure 7). This compensation may in part be mediated by *Otx1* (Acampora et al., 1997; Suda et al., 1997), which is expressed at low levels in the MGE (Figure S1).

Otx2 regulates rostrocaudal and dorsoventral patterning of the MGE

There is evidence that vMGE generates most of the GP, whereas the dMGE may principally generate interneurons (Flandin et al., 2010). Whereas *Nkx2.1* function is required throughout the MGE (Sussel et al., 1999; Flandin et al., 2010), *Otx2* preferentially controls the identity of the vMGE. This is a surprising result, given that *Otx2* mRNA and protein are expressed throughout the MGE.

Analysis of gene expression changes and OTX2 genomic binding sites provides three lines of evidence that *Otx2* specifies vMGE identity through direct regulation of TF genes expressed in the vMGE and POA (Figure S7): 1) *Otx2* autoregulates its transcription in the MGE and POA (Figure 1, 2); 2) *Otx2* drives vMGE expression of *Sall3, Tal2* and *Tll2* (Figure 6; Table S1). OTX2 has binding sites near these genes (Figures 2, S5); 3) *Otx2* represses POA identity in the MGE by blocking *Dbx1*, *Slit2* and *Sox3* expression (Figure 6 and not shown). There is OTX2 binding near *Dbx1* (Figure 2). Note that *Nkx2.1* expression persists in vMGE progenitors in *Otx2* mutants (Figure 7J–L); thus *Otx2* and *Nkx2.1* may specify vMGE identity via parallel pathways.

vMGE respecification in *Otx2* mutants has consequences for subpallial development, including GP agenesis (or, loss of molecular identity based on *ER81*, *Lhx6*, *Lhx8*, *Nkx2.1*, *Zic1*; Figures 7, S4). There is dorsal and rostral expansion of POA progenitor (*Arhgap22*, *Dbx1*, *Slit2*, *Sox3*), and neuronal (*Nkx5.2* and *Sox14*), properties (Figures 6, 7). Other vMGE neuronal cell types are reduced, including *Lhx6*^{+} neurons in the ventral pallidum, and cholinergic neurons in the nucleus basalis, diagonal band and striatum (ChAT[+], *Lhx8*^{+}, and *TrkA*[+]; Figure S4).

Otx2 also impacts patterning of the telencephalon along the rostrocaudal axis. RPC Fgf expression domains are expanded rostrally by E11.5 in *Otx2* mutants (Figure 3). *COUP-TF1*, a TF expressed in the caudal MGE, is repressed by *Otx2*, as *COUP-TF1* is ectopically expressed rostrally by E13.5 in the mutants (Figure 6). In addition, several POA markers expand rostrally as well as dorsally into the MGE (*Nkx5.2*, *Dbx1*; Figure 6). Thus, *Otx2* controls both rostrocaudal and dorsoventral MGE patterning.

In summary, *Otx2* is essential in the E8.5–E13.5 telencephalon for regional specification of the RPC and vMGE, and for MGE neurogenesis and oligodendrogenesis. In the absence of *Otx2*, the RPC takes on MHB properties and the vMGE takes on POA properties, leading to Se, GP and cholinergic deficits. OTX2 ChIP-seq provided evidence for direct mechanisms through which *Otx2* controls regional and cell type identity in the subpallium.

EXPERIMENTAL PROCEDURES

Mouse lines

We used the following published mouse lines: *Fgf8^neo* (G. Martin, UCSF; (Meyers et al., 1998), non-hypomorphic *Otx2^f* (S. Aizawa, CDB, RIKEN; Acc. No. CDB0013K, http://www.cdb.riken.jp/arg/mutant%20mice%20list.html; (Tian et al., 2002)), *RxCre* (Y. Zhao, NIH; (Swindell et al., 2006)), *Nkx2.1Cre* (Stewart Anderson, U. Penn. (Xu et al., 2008)), *Fgf8^CreER* (Hoch et al, manuscript in preparation). *Otx2^{f/+}* mice were crossed to *βactin::Cre* (Lewandoski et al., 1997) to generate *Otx2^{+/−}* mice. Unless otherwise specified, conditional knockouts were of the genotype *Otx2^{f/−}; Cre^+*, generated by crossing *Otx2^{f/f}* mice to Cre lines maintained on an *Otx2^{+/−}* background. Mice were maintained in social cages in a specific pathogen-free barrier facility at UCSF on a 12 hour light/dark cycle with free access to food and water.

For embryonic (timed mating) experiments, day 0.5 was designated as noon on the day a vaginal plug was observed. At the time of experiment, mice were euthanized by CO2 inhalation followed by cervical dislocation. Embryonic heads (E10.5–E12.5) or isolated brains (E13.5 and older) were fixed overnight in 4% PFA (made in 1x PBS), transferred to 30% sucrose for cryoprotection, and then embedded and frozen in OCT for cryosectioning. Section thickness ranged from 10–20 μm depending on stage.

For postnatal experiments (>P7), animals were anesthetized with i.p. avertin (0.015 ml/g of 2.5% solution), perfused transcardially with 1X PBS and with 4% PFA, followed by brain isolation, fixation, cryoprotection, and freezing/embedding.

Immunohistochemistry (IHC)

We used the following antibodies: ChAT (Chemicon AB144P), Otx2 (R&D systems goat, catalog # AF1979), Tuj1 (Covance MMS-435P), pH3 (Millipore 06-570), parvalbumin (Millipore MAB1572), somatostatin (Santa Cruz sc-7819).

Cryosections were rinsed in PBS, blocked in 10% normal serum/PBST (1x PBS, 0.1% Triton X-100), incubated in primary antibody overnight (4° C), washed in PBST, incubated in secondary antibody 1–3 hours (room temperature), and washed in PBS. For fluorescent detection, we used Alexa 488- and Alexa 594-conjugated secondary antibodies (Invitrogen). For colorimetric detection, biotinylated secondary antibodies (Vector) were used with the ABC (Vector)/DAB detection method.

For ChAT IHC, antigen retrieval was achieved by incubating slides in 2.94g/L trisodium citrate dehydrate, 0.05% Tween-20, pH 6.0 for 15 minutes at 90° C. Blocking and antibody incubations were done in 1% BSA in PBST. Sections were incubated two days at 4° C with primary antibody, and signal was amplified with biotinylated anti-goat (Vector) prior to fluorescent detection with streptavidin-594 (Invitrogen).

For OTX2 IHC, we modified the IHC protocol according to the recommendations of Yuki Muranishi in the Furakawa lab (Osaka, Japan). Briefly, antigen retrieval was achieved as for ChAT IHC, and samples were blocked in 4% donkey serum in PBST.

In situ hybridization (ISH)

We performed ISH on a minimum of n=2 and n=3 biological replicates for controls and mutants, respectively. In each case, a rostrocaudal series of at least 10 sections was examined. Reduced expression was interpreted as reduced RNA per cell, unless otherwise stated. Section ISHs were performed using digoxigenin-labeled riboprobes as described (Schaeren-Wiemers and Gerfin-Moser, 1993) with the following modifications. Prior to acetylation, sections were incubated with proteinase K (1μg/ml) and post-fixed in 4% PFA. Slides were equilibrated in NTT prior to antibody incubation (overnight, 4° C, AP-antidigoxigenin (Roche)), and then washed in NTT 3 x 30 minutes at room temperature. They were then washed 3 times in NTTML (NTT + 50 mM MgCl$_2$, 2 mM Levamisole) and transferred to BM Purple (Roche) for colorimetric detection (dark, 37° C). Slides were rinsed in water, then postfixed (4% PFA overnight), dehydrated, incubated briefly in xylene, and coverslipped using Permount. *Acetylation buffer:* 1.33% (v/v) triethanolamine, 0.065% HCl, 0.375% (v/v) acetic anhydride. *Riboprobe block/hybridization buffer:* 50% formamide, 5x SSC pH 4.5, 1% SDS, 50 μg/ml yeast tRNA, 50 μg/ml heparin. *Antibody blocking buffer (NTT):* 0.15M NaCl, 0.1M Tris pH 8.0, 0.1% Tween-20.

E12.5 RNA isolation and microarray

Subpallial (GE and Se) tissue was microdissected from E12.5 female brains (n=4 control, n=3 CKO), snap frozen, and stored at −80°C. Total RNA was isolated using the Qiagen RNAeasy kit. RNA was amplified (labeled with Cy3-CTP) with Agilent low RNA input fluorescent linear amplification kits, and cRNA was assessed using the Nandrop ND-100 (Nanodrop Technologies, Inc., Wilmington DE). Equal amounts of Cy3 labeled target were hybridized to Agilent whole mouse genome 4x44K Ink-jet arrays, by the UCSF Genomics Core, who then performed the differential gene expression analysis (http://www.arrays.ucsf.edu; http://www.agilent.com) (Holm, 1979) Bolstad et al., 2003; Gentleman et al., 2004; Smyth, 2004). Significant changes in gene expression were defined as B value greater than zero. B = log 10 posterior odds ratio, ratio between the probability that a given gene is differentially expressed (DE) over the probability that a given gene is not differentially expressed. B   0 means equal or greater probability that a gene is DE than non-DE (Lonnstedt and Speed, 2002).

Chromatin immunoprecipitation-sequencing experiment (ChIP-seq) and informatics

ChIP was performed using anti-OTX2 (R&D #AF1979) (McKenna et al., 2011). E12.5 CD1 GEs were fixed in 1.5% formaldehyde for 20 min. and neutralized with glycine. Fixed chromatin was lysed and sheared into 200–1000 bp fragments using a bioruptor (Diagenode). Immunoprecipitation (IP) reactions were performed in duplicates using Goat IgG as negative controls. Precipitated fractions were purified using Dynabeads (Invitrogen). Libraries were prepared using an Ovation Ultralow DR Multiplex System (Nugen), size selected in the range of 200–300 bp on a LabChip (Lifesciences), quality control tested on a Bioanalyzer (Agilent) and sequenced on a HiSeq (Illumina). Reads from ChIP, input, and negative control (IgG) libraries were mapped to the mouse genome (mm9) using BWA and peaks were called using MACS considering both input and IgG as the control sample with filtering to remove peaks in repeat regions.

For downstream analysis of ChIP-seq data, only peaks that overlapped in each of the 3 OTX2 ChIP-seq replicates were selected (590 regions). Nucleotide motifs were identified using the Regulatory Sequence Analysis Tools (RSAT) peak-motifs tool (Thomas-Chollier et al., 2011). Gene Ontology for biological process and molecular function was computed using the Genomic Regions Enrichment of Annotations Tool (GREAT) (McLean et al., 2010).

Supplementary Material

Refer to Web version on PubMed Central for supplementary material.

Acknowledgments

References

Acampora D, Avantaggiato V, Tuorto F, Simeone A. Genetic control of brain morphogenesis through Otx gene dosage requirement. Development. 1997; 124(18):3639–50. [PubMed: 9342056]

Acampora D, Mazan S, Lallemand Y, Avantaggiato V, Maury M, Simeone A, Brulet P. Forebrain and midbrain regions are deleted in Otx2–/– mutants due to a defective anterior neuroectoderm specification during gastrulation. Development. 1995; 121(10):3279–90. [PubMed: 7588062]

Acampora D, Simeone A. The TINS Lecture. Understanding the roles of Otx1 and Otx2 in the control of brain morphogenesis. Trends Neurosci. 1999; 22(3):116–22. [PubMed: 10199636]

Ahituv N, Zhu Y, Visel A, Holt A, Afzal V, Pennacchio LA, Rubin EM. Deletion of ultraconserved elements yields viable mice. PLoS Biol. 2007; 5(9):e234. [PubMed: 17803355]

Ang SL, Jin O, Rhinn M, Daigle N, Stevenson L, Rossant J. A targeted mouse Otx2 mutation leads to severe defects in gastrulation and formation of axial mesoderm and to deletion of rostral brain. Development. 1996; 122(1):243–52. [PubMed: 8565836]

Asbreuk CH, van Schaick HS, Cox JJ, Kromkamp M, Smidt MP, Burbach JP. The homeobox genes Lhx7 and Gbx1 are expressed in the basal forebrain cholinergic system. Neuroscience. 2002; 109(2):287–98. [PubMed: 11801365]

Assimacopoulos S, Kao T, Issa NP, Grove EA. Fibroblast growth factor 8 organizes the neocortical area map and regulates sensory map topography. J Neurosci. 2012; 232(21):7191–7201. [PubMed: 22623663]

Batista-Britto, R.; Fishell, G. The generation of cortical interneurons. In: Rubenstein, JLR.; Rakic, P., editors. Patterning and Cell Type Specification in the Developing CNS and PNS. Vol. 1. Academic Press; San Diego, CA: 2013.

Bolstad BM, Irizarry RA, Astrand M, Speed TP. A comparison of normalization methods for high density oligonucleotide array data based on variance and bias. Bioinformatics. 2003; 19(2):185–93. [PubMed: 12538238]

Casarosa S, Fode C, Guillemot F. Mash1 regulates neurogenesis in the ventral telencephalon. Development. 1999; 126(3):525–34. [PubMed: 9876181]

Chi CL, Martinez S, Wurst W, Martin GR. The isthmic organizer signal FGF8 is required for cell survival in the prospective midbrain and cerebellum. Development. 2003; 130(12):2633–44. [PubMed: 12736208]

Cholfin JA, Rubenstein JLR. Patterning of frontal cortex subdivisions by Fgf17. Proc Natl Acad Sci U S A. 2007; 104:7652–7657. [PubMed: 17442747]

Colasante G, Collombat P, Raimondi V, Bonanomi D, Ferrai C, Maira M, Yoshikawa K, Mansouri A, Valtorta F, Rubenstein JL, Broccoli V. Arx is a direct target of Dlx2 and thereby contributes to the tangential migration of GABAergic interneurons. J Neurosci. 2008; 28(42):10674–86. [PubMed: 18923043]

Crossley PH, Martinez S, Ohkubo Y, Rubenstein JL. Coordinate expression of Fgf8, Otx2, Bmp4, and Shh in the rostral prosencephalon during development of the telencephalic and optic vesicles. Neuroscience. 2001; 108(2):183–206. [PubMed: 11734354]

Eswarakumar VP, Lax I, Schlessinger J. Cellular signaling by fibroblast growth factor receptors. Cytokine & growth factor reviews. 2005; 16(2):139–49. [PubMed: 15863030]

Faedo A, Borello U, Rubenstein JL. Repression of Fgf signaling by sprouty1-2 regulates cortical patterning in two distinct regions and times. J Neurosci. 2010; 30(11):4015–23. [PubMed: 20237272]

Flames N, Pla R, Gelman DM, Rubenstein JL, Puelles L, Marin O. Delineation of multiple subpallial progenitor domains by the combinatorial expression of transcriptional codes. The Journal of neuroscience : the official journal of the Society for Neuroscience. 2007; 27(36):9682–95. [PubMed: 17804629]

Flandin P, Kimura S, Rubenstein JL. The progenitor zone of the ventral medial ganglionic eminence requires Nkx2-1 to generate most of the globus pallidus but few neocortical interneurons. J Neurosci. 2010; 30(8):2812–23. [PubMed: 20181579]

Fukuchi-Shimogori T, Grove EA. Neocortex patterning by the secreted signaling molecule FGF8. Science. 2001; 294(5544):1071–4. [PubMed: 11567107]

Ghanem N, Yu M, Long J, Hatch G, Rubenstein JL, Ekker M. Distinct cis-regulatory elements from the Dlx1/Dlx2 locus mark different progenitor cell populations in the ganglionic eminences and different subtypes of adult cortical interneurons. J Neurosci. 2007; 27(19):5012–22. [PubMed: 17494687]

Garel S, Huffman KJ, Rubenstein JL. Molecular regionalization of the neocortex is disrupted in Fgf8 hypomorphic mutants. Development. 2003; 130(9):1903–14. [PubMed: 12642494]

Gelman D, Griveau A, Dehorter N, Teissier A, Varela C, Pla R, Pierani A, Marin O. A wide diversity of cortical GABAergic interneurons derives from the embryonic preoptic area. The Journal of neuroscience : the official journal of the Society for Neuroscience. 2011; 31(46):16570–80. [PubMed: 22090484]

Gentleman RC, Carey VJ, Bates DM, Bolstad B, Dettling M, Dudoit S, Ellis B, Gautier L, Ge Y, Gentry J, et al. Bioconductor: open software development for computational biology and bioinformatics. Genome biology. 2004; 5(10):R80. [PubMed: 15461798]

Goulding MD, Chalepakis G, Deutsch U, Erselius JR, Gruss P. Pax-3, a novel murine DNA binding protein expressed during early neurogenesis. The EMBO journal. 1991; 10(5):1135–47. [PubMed: 2022185]

Grove, EA.; Monucki, ES. Morphogens, patterning centers, and their mechanisms of action. In: Rubenstein, JLR.; Rakic, P., editors. Patterning and Cell Type Specification in the Developing CNS and PNS. Vol. 1. Academic Press; San Diego, CA: 2013.

Hirata T, Li P, Lanuza GM, Cocas LA, Huntsman MM, Corbin JG. Identification of distinct telencephalic progenitor pools for neuronal diversity in the amygdala. Nature neuroscience. 2009; 12(2):141–9. [PubMed: 19136974]

Hoch RV, Clarke JA, Rubenstein JL. Fgf Signaling Controls the Telencephalic Distribution of Fgf-Expressing Progenitors Generated in the Rostral Patterning Center. Neural Development. 2015; 10:8. in press. 10.1186/s13064-015-0037-7 [PubMed: 25889070]

Holm S. A simple sequentially rejective multiple test procedure. Scandinavian Journal of Statistics. 1979; 6:65–70.

Jeong Y, El-Jaick K, Roessler E, Muenke M, Epstein DJ. A functional screen for sonic hedgehog regulatory elements across a 1 Mb interval identifies long-range ventral forebrain enhancers. Development. 2006; 133(4):761–772. [PubMed: 16407397]

Joyner AL, Liu A, Millet S. Otx2, Gbx2 and Fgf8 interact to position and maintain a mid-hindbrain organizer. Current opinion in cell biology. 2000; 12(6):736–41. [PubMed: 11063941]

Kessaris N, Fogarty M, Iannarelli P, Grist M, Wegner M, Richardson WD. Competing waves of oligodendrocytes in the forebrain and postnatal elimination of an embryonic lineage. Nature neuroscience. 2006; 9(2):173–9. [PubMed: 16388308]

Kurokawa D, Kiyonari H, Nakayama R, Kimura-Yoshida C, Matsuo I, Aizawa S. Regulation of Otx2 expression and its functions in mouse forebrain and midbrain. Development. 2004a; 131(14): 3319–31. [PubMed: 15201224]

Kurokawa D, Takasaki N, Kiyonari H, Nakayama R, Kimura-Yoshida C, Matsuo I, Aizawa S. Regulation of Otx2 expression and its functions in mouse epiblast and anterior neuroectoderm. Development. 2004b; 131(14):3307–17. [PubMed: 15201223]

Lewandoski M, Meyers EN, Martin GR. Analysis of Fgf8 gene function in vertebrate development. Cold Spring Harb Symp Quant Biol. 1997; 62:159–68. [PubMed: 9598348]

Liu A, Joyner AL. EN and GBX2 play essential roles downstream of FGF8 in patterning the mouse mid/hindbrain region. Development. 2001; 128(2):181–91. [PubMed: 11124114]

Lonnstedt I, Speed TP. Replicated microarray data. Stat Sinica. 2002; 2:31–46.

Martinez S, Crossley PH, Cobos I, Rubenstein JL, Martin GR. FGF8 induces formation of an ectopic isthmic organizer and isthmocerebellar development via a repressive effect on Otx2 expression. Development. 1999; 126(6):1189–200. [PubMed: 10021338]

Matsunaga E, Araki I, Nakamura H. Role of Pax3/7 in the tectum regionalization. Development. 2001; 128(20):4069–77. [PubMed: 11641229]

McKenna WL, Betancourt J, Larkin KA, Abrams B, Guo C, Rubenstein JL, Chen B. Tbr1 and Fezf2 regulate alternate corticofugal neuronal identities during neocortical development. The Journal of neuroscience : the official journal of the Society for Neuroscience. 2011; 31(2):549–64. [PubMed: 21228164]

McLean CY, Bristor D, Hiller M, Clarke SL, Schaar BT, Lowe CB, Wenger AM, Bejerano G. GREAT improves functional interpretation of *cis*-regulatory regions. Nat Biotechnol. 2010; 28(5):495–501. [PubMed: 20436461]

Meyers EN, Lewandoski M, Martin GR. An Fgf8 mutant allelic series generated by Cre- and Flp-mediated recombination. Nat Genet. 1998; 18(2):136–41. [PubMed: 9462741]

Minowada G, Jarvis LA, Chi CL, Neubuser A, Sun X, Hacohen N, Krasnow MA, Martin GR. Vertebrate Sprouty genes are induced by FGF signaling and can cause chondrodysplasia when overexpressed. Development. 1999; 126(20):4465–75. [PubMed: 10498682]

Petryniak MA, Potter GB, Rowitch DH, Rubenstein JL. Dlx1 and Dlx2 control neuronal versus oligodendroglial cell fate acquisition in the developing forebrain. Neuron. 2007; 55(3):417–33. [PubMed: 17678855]

Puelles E, Acampora D, Lacroix E, Signore M, Annino A, Tuorto F, Filosa S, Corte G, Wurst W, Ang SL, et al. Otx dose-dependent integrated control of antero-posterior and dorso-ventral patterning of midbrain. Nature neuroscience. 2003; 6(5):453–60. [PubMed: 12652306]

Rhinn M, Dierich A, Shawlot W, Behringer RR, Le Meur M, Ang SL. Sequential roles for Otx2 in visceral endoderm and neuroectoderm for forebrain and midbrain induction and specification. Development. 1998; 125(5):845–56. [PubMed: 9449667]

Rubenstein, JLR.; Campbell, K. Neurogenesis in the basal ganglia. In: Rubenstein, JLR.; Rakic, P., editors. Patterning and Cell Type Specification in the Developing CNS and PNS. Vol. 1. Academic Press; San Diego, CA: 2013.

Sakurai Y, Kurokawa D, Kiyonari H, Kajikawa E, Suda Y, Aizawa S. Otx2 and Otx1 protect diencephalon and mesencephalon from caudalization into metencephalon during early brain regionalization. Developmental biology. 2010; 347(2):392–403. [PubMed: 20816794]

Sanchez-Ortiz E, Yui D, Song D, Li Y, Rubenstein JL, Reichardt LF, Parada LF. TrkA gene ablation in basal forebrain results in dysfunction of the cholinergic circuitry. The Journal of neuroscience : the official journal of the Society for Neuroscience. 2012; 32(12):4065–79. [PubMed: 22442072]

Schaeren-Wiemers N, Gerfin-Moser A. A single protocol to detect transcripts of various types and expression levels in neural tissue and cultured cells: in situ hybridization using digoxigenin-labelled cRNA probes. Histochemistry. 1993; 100(6):431–40. [PubMed: 7512949]

Silbereis JC, Nobuta H, Tsai HH, Heine VM, McKinsey GL, Meijer DH, Howard MA, Petryniak MA, Potter GB, Alberta JA, et al. Olig1 function is required to repress dlx1/2 and interneuron production in Mammalian brain. Neuron. 2014; 81(3):574–87. [PubMed: 24507192]

Simeone A. Positioning the isthmic organizer where Otx2 and Gbx2meet. Trends in genetics : TIG. 2000; 16(6):237–40. [PubMed: 10827447]

Simeone A, Acampora D, Gulisano M, Stornaiuolo A, Boncinelli E. Nested expression domains of four homeobox genes in developing rostral brain. Nature. 1992; 358(6388):687–90. [PubMed: 1353865]

Smyth GK. Linear models and empirical bayes methods for assessing differential expression in microarray experiments. Statistical applications in genetics and molecular biology. 2004; 3:Article 3.

Storm EE, Garel S, Borello U, Hebert JM, Martinez S, McConnell SK, Martin GR, Rubenstein JL. Dose-dependent functions of Fgf8 in regulating telencephalic patterning centers. Development. 2006; 133(9):1831–44. [PubMed: 16613831]

Suda Y, Matsuo I, Aizawa S. Cooperation between Otx1 and Otx2 genes in developmental patterning of rostral brain. Mechanisms of development. 1997; 69(1–2):125–41. [PubMed: 9486536]

Suda Y, Matsuo I, Kuratani S, Aizawa S. Otx1 function overlaps with Otx2 in development of mouse forebrain and midbrain. Genes to cells : devoted to molecular & cellular mechanisms. 1996; 1(11): 1031–44. [PubMed: 9077465]

Sussel L, Marin O, Kimura S, Rubenstein JL. Loss of Nkx2.1 homeobox gene function results in a ventral to dorsal molecular respecification within the basal telencephalon: evidence for a transformation of the pallidum into the striatum. Development. 1999; 126(15):3359–70. [PubMed: 10393115]

Swindell EC, Bailey TJ, Loosli F, Liu C, Amaya-Manzanares F, Mahon KA, Wittbrodt J, Jamrich M. Rx-Cre, a tool for inactivation of gene expression in the developing retina. Genesis. 2006; 44(8): 361–3. [PubMed: 16850473]

Thisse B, Thisse C. Functions and regulations of fibroblast growth factor signaling during embryonic development. Developmental biology. 2005; 287(2):390–402. [PubMed: 16216232]

Tian E, Kimura C, Takeda N, Aizawa S, Matsuo I. Otx2 is required to respond to signals from anterior neural ridge for forebrain specification. Dev Biol. 2002; 242(2):204–23. [PubMed: 11820816]

Thomas-Chollier M, Herrmann C, Defrance M, Sand O, Thieffry D, van Helden J. RSAT peak-motifs: motif analysis in full-size ChIP-seq datasets. Nucleic Acids Research. 2011:9.10.1093/nar/gkr1104

Vernay B, Koch M, Vaccarino F, Briscoe J, Simeone A, Kageyama R, Ang SL. Otx2 regulates subtype specification and neurogenesis in the midbrain. The Journal of neuroscience : the official journal of the Society for Neuroscience. 2005; 25(19):4856–67. [PubMed: 15888661]

Waclaw RR, Ehrman LA, Pierani A, Campbell K. Developmental origin of the neuronal subtypes that comprise the amygdalar fear circuit in the mouse. The Journal of neuroscience : the official journal of the Society for Neuroscience. 2010; 30(20):6944–53. [PubMed: 20484636]

Xu Q, Tam M, Anderson SA. Fate mapping Nkx2.1-lineage cells in the mouse telencephalon. J Comp Neurol. 2008; 506(1):16–29. [PubMed: 17990269]

Yun K, Fischman S, Johnson J, Hrabe de Angelis M, Weinmaster G, Rubenstein JL. Modulation of the notch signaling by Mash1 and Dlx1/2 regulates sequential specification and differentiation of progenitor cell types in the subcortical telencephalon. Development. 2002; 129(21):5029–5040. [PubMed: 12397111]

Zhang Y, Miki T, Iwanaga T, Koseki Y, Okuno M, Sunaga Y, Ozaki N, Yano H, Koseki H, Seino S. Identification, tissue expression, and functional characterization of Otx3, a novel member of the Otx family. J Biol Chem. 2002; 277(31):28065–28069. [PubMed: 12055180]

Highlights

- OTX2 directs enhancer regulation.

- *Otx2* regulates *Fgf8* expression and Fgf signaling responses.

- *Otx2* promotes MGE neurogenesis and oligodendrogenesis.

- *Otx2* is required for specification of vMGE versus POA fate.
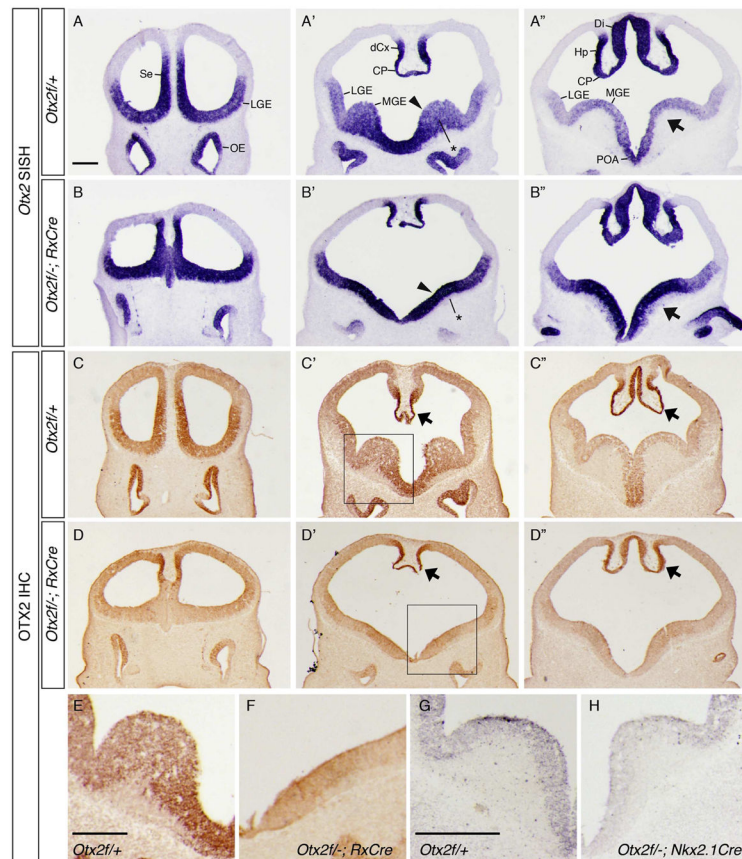
Figure 1. Otx2 expression in conditional knock outs (cKOs)

(A-B") ISH on E11.5 coronal sections from (A–A") *Otx2f/+* and (B–B") *Otx2f/−; RxCre* embryos using a full length *Otx2* riboprobe. Otx2 transcription appears upregulated in the MGE of *RxCre* cKOs (arrowheads and arrows in A', A", B', B"), and that the MGE SVZ and MZ are hypoplastic (asterisks in A', B'). (C–H) Anti-OTX2 IHC: in *RxCre* cKOs (C–F), OTX2 protein expression is absent in cKO forebrains except in the dorsomedial caudal cortex, hippocampal anlage, and choroid plexus (arrows, C'-C", D'–D"). E and F show higher magnification views of the boxed regions in C', D'. (G–H) In *Nkx2.1Cre* cKOs, OTX2 expression was reduced in the MGE. A–D": rostrocaudal series of coronal sections. Abbreviations: Se, septum; MGE, medial ganglionic eminence; LGE, lateral ganglionic eminence; dCx, dorsomedial cortex; Hp, hippocampal anlage; POA, preoptic area; Di, diencephalon; CP, choroid plexus; OE, olfactory epithelium. *Scale bars: A, E = 0.25mm, G = 0.4mm.*
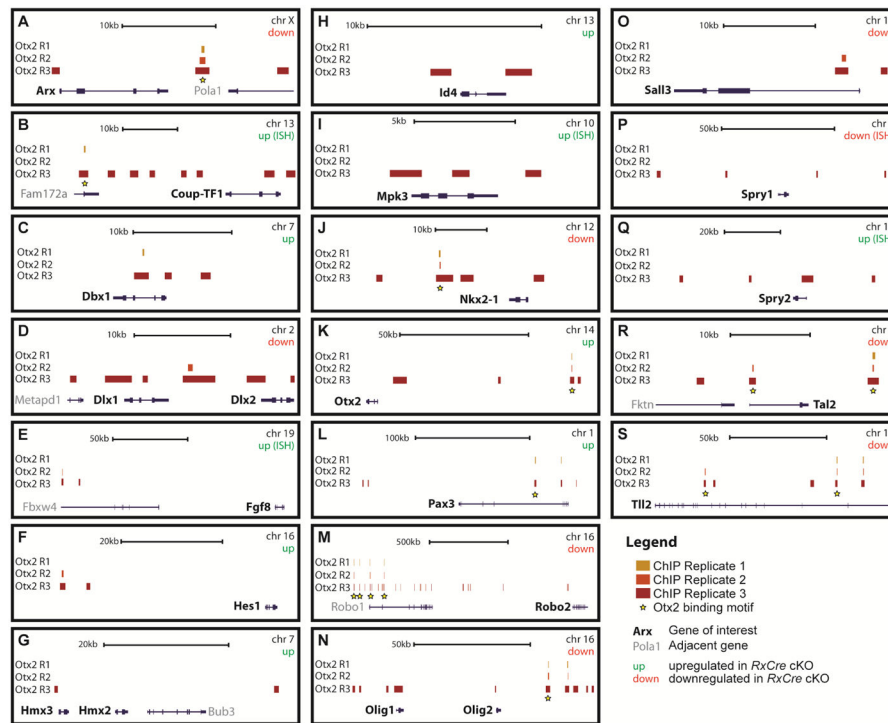
Figure 2. Anti-OTX2 ChIP-seq results

"Called" peak locations relative to genomic loci are shown for genes (alphabetically organized) that are deregulated in *Otx2* cKOs, and for which ChIP-seq peaks were identified within ~1 megabase (MB) of the gene body. Note the different scale bars for individual panels. Black arrows and text identify the *Otx2*-regulated gene of interest, grey arrows and text designate nearby genes. For each panel, italicized "up" or "down" indicates whether the gene was upregulated or downregulated in *RxCre* cKO forebrains. The yellow stars indicate that the OTX2-ChIP-seq peak had an OTX2 binding motif. Abbreviations: chr: chromosome; kb: kilobase
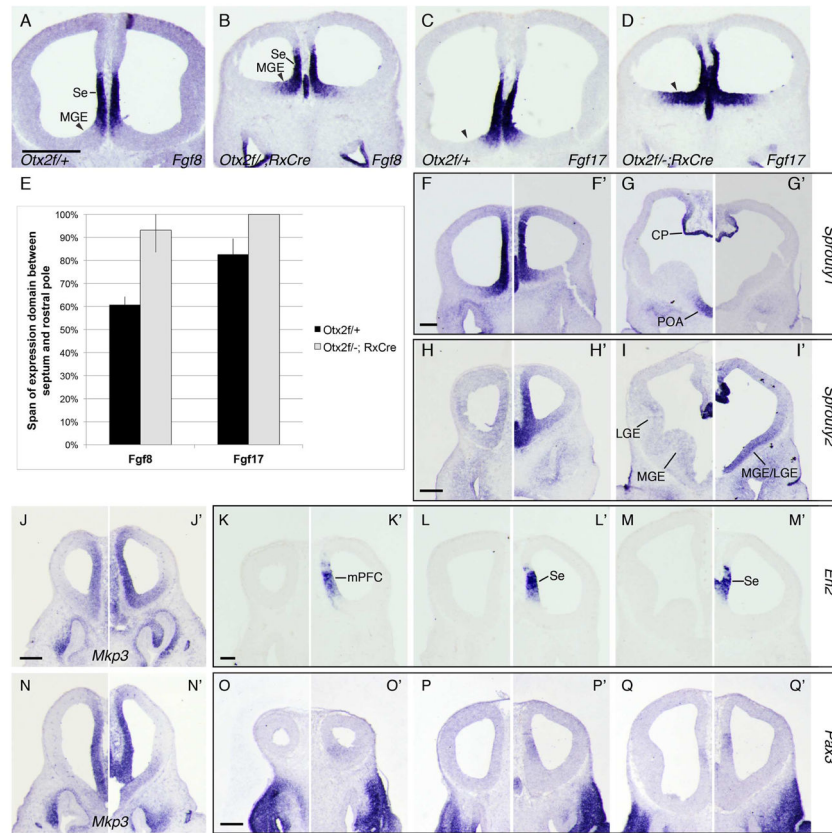
Figure 3. *Otx2* restricts the domain of *Fgf* expression and controls regional specification of the RPC

(A–D, F–Q') ISH comparing gene expression in (A, C, F–Q) *Otx2f/+* and (B, D, F'–Q') *Otx2f/-; RxCre* embryos at E11.5. (A–B) *Fgf8*, (C–D) *Fgf17*, (F–G') *Sprouty1*, (H–I') *Sprouty2*, (J–J', N-N') *Mkp3*, (K–M') *En2*, (O–Q') *Pax3*. (E) Quantification of the rostral expansion of *Fgf* expression in cKO and control embryos at E11.5 (mean +/− st. dev.). For each embryo, we calculated the distance from the caudal septum (where Fgf8 and Fgf17 are expressed) to the rostral limit of Fgf expression, and expressed this as a percentage of the total (rostral telencephalic pole > caudal septum) distance. Rostral expansion was statistically significant for Fgf8 ($p < 0.001$) but not Fgf17 ($p = 0.17$; 2-tailed t tests, unequal variance). Abbreviation: mPFC, medial prefrontal cortex. *Scale bars: A–D = 0.5mm, F–G' = 0.2mm, H–Q' = 0.25mm.*
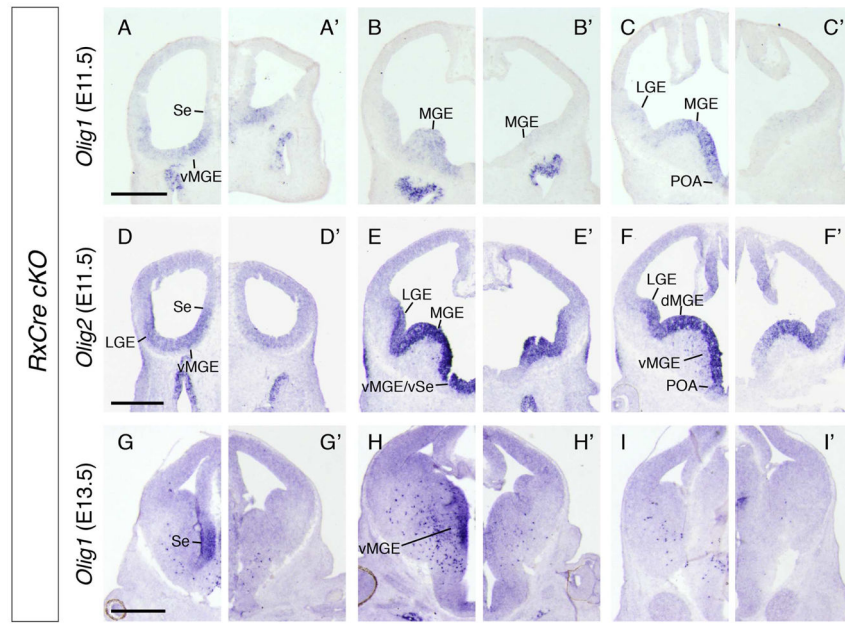
Figure 4. *Otx2* cKOs exhibit deficits in molecular markers of oligodendrogenesis
ISH on coronal hemisections from (A–I) *Otx2f/+*, (A'–I') *Otx2f/−; RxCre*, embryos: (A–C')
Olig1 at E11.5, (D–F') *Olig2* at E11.5, (G–I') *Olig1* at E13.5. Three planes of section are
shown along the rostral-caudal axis. Abbreviations: vMGE, ventral MGE; dMGE, dorsal
MGE; vSe, ventral septum. *Scale bars: A–F' = 0.5mm, G–I' = 0.4mm.*
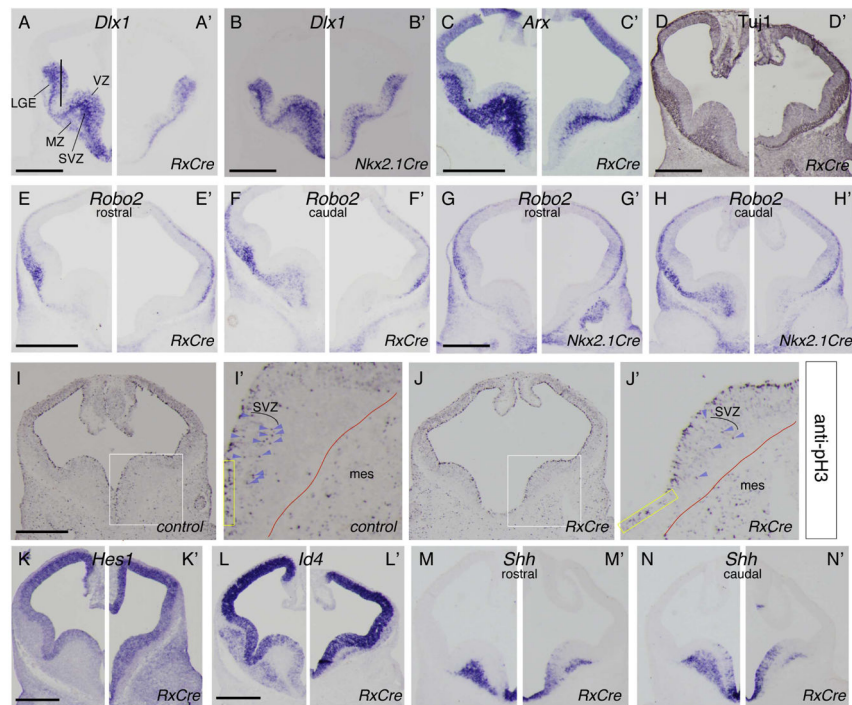
Figure 5. Reduced neurogenesis and proliferation in the basal ganglia of E11.5 *Otx2* cKOs
ISH and IHC on coronal hemisections (control: left, mutant: right). (A–H') ISH: (A–H)
Otx2f/+, (A', C', D'–F') *Otx2f/−; RxCre*, and (B', G'–H') *Otx2f/−; Nkx2.1Cre* embryos
using probes to (A–B') *Dlx1*, (C–C') *Arx*, (E–H') *Robo2*. Anti-Tuj1 IHC (D) *Otx2f/+* and
(D') *Otx2f/−; RxCre*. (I–J') Anti- pH3 IHC: (I', I) *Otx2f/+* and (J, J') *Otx2f/−; RxCre*
embryos. I'–J': high magnification of I, J. Red lines: neural/mesenchymal boundary; purple
arrowheads: pH3+ SVZ cells; yellow rectangles highlight similar VZ regions of the vMGE
in K–L' showing upregulation of *Hes1* and *Id4,* respectively. (K, L) *Otx2f/+* and (K', L')
Otx2f/-; RxCre embryos. (M–N') *Shh* reduction in MZ and increase in VZ. Abbreviations:
mes: mesenchyme; SVZ: subventricular zone; VZ ventricular zone. *Scale bars: 0.5mm.*
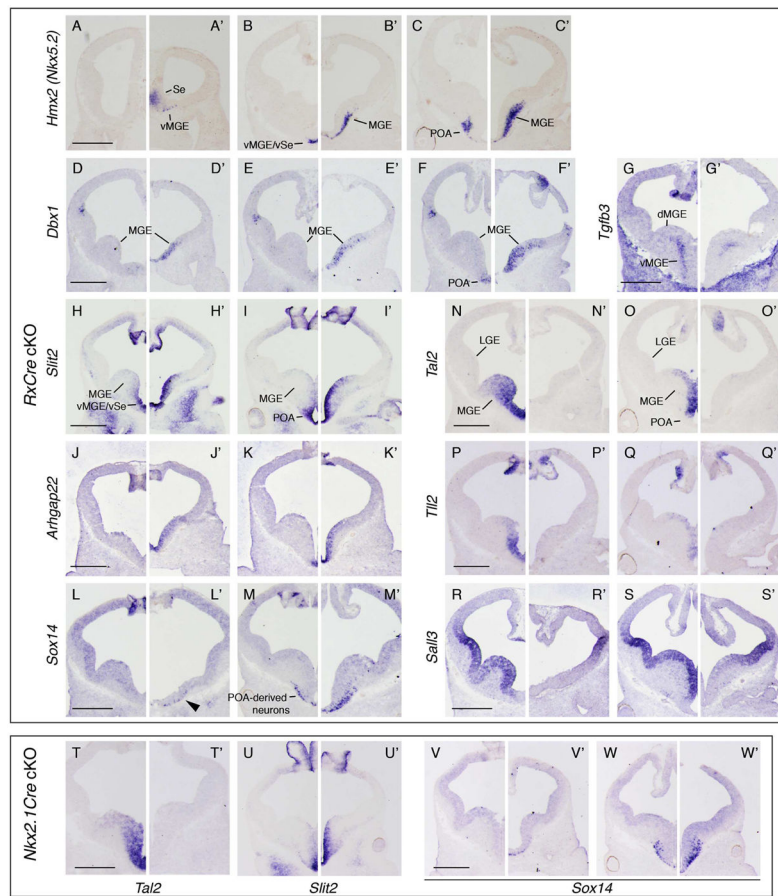
Figure 6. Re-specification of the vMGE towards the POA fate in *Otx2 RxCre* cKOs
ISH on E11.5 coronal hemisections from (A–S) *Otx2f/+*, (A'–O') *Otx2f/−; RxCre*, and
(P'S') *Otx2f/−; Nkx2.1Cre* embryos showing expanded expression of POA genes (A–M', U–
W') and diminished expression of vMGE genes (N–S', T–T') in cKOs. For each experiment
(except *Tal2* and *Slit2* in *Nkx2.1Cre cKOs*), two or three sections are shown to demonstrate
effects at different rostral-caudal planes. (A–C') *Hmx2* (*Nkx5.2*), (D–F') *Dbx1*, (G–G')
Tgfb3, (H–I', U–U') *Slit2*, (J–K') *Arhgap22*, (L–M', V–W') *Sox14*, (N–O', T–T') *Tal2*, (P–
Q') *Tll2*, (R–S') *Sall3*. Scale bars: 0.5mm.
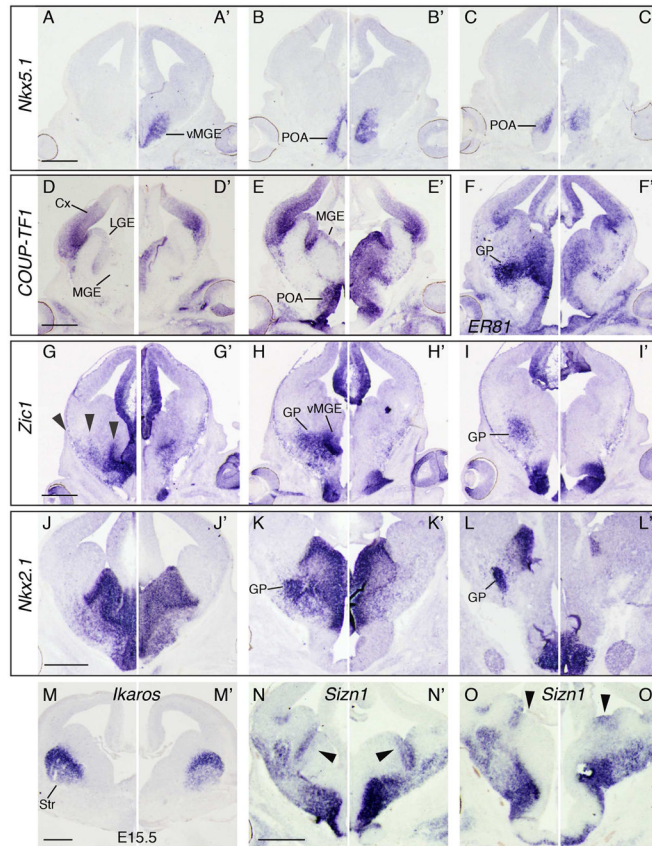
Figure 7. E13.5-E15.5 MGE and POA development in *Otx2* cKOs. ISH on (A–O)
Otx2f/+ and (A'–O') *Otx2f/−; RxCre* coronal hemisections, using the following probes:
(AC') *Nkx5.1*, (D–E') *COUP-TF1*, (F–F') *ER81*, (G–I') *Zic1*, (J–L') *Nkx2.1*, (M–M')
Ikaros, (NO') *Sizn1*. Arrowheads in G indicate three streams of neurons or progenitors that
appear to emanate from the POA or vMGE and migrate toward the MGE, LGE, and ventral
cortex; these streams are not apparent in cKOs. Arrowheads in N–O' point to the dMGE:
Sizn1 expression appears to shift ventrally from its vLGE domain into the dMGE in cKOs.
All are E13.5 except for *Ikaros*, which is E15.5. Note that in L', the dark region in the CGE
(*) is a tissue fold, not ISH signal. Abbreviations: GP, globus pallidus; Str, striatum. *Scale bars: 0.5mm.*